Particle-core multiplets in ^{97}Mo populated via the (^{3}He,2nγ) reaction

K. D. Carnes,* F. A. Rickey, G. S. Samudra,† and P. C. Simms
Tandem Accelerator Laboratory, Purdue University, Lafayette, Indiana 47907
(Received 15 September 1986)

^{97}Mo nuclei were produced by the ^{96}Zr(^{3}He,2nγ)^{97}Mo reaction at 11 MeV. Excitation functions, angular distributions, linear polarizations, and gamma-gamma coincidences were measured and used to construct a ^{97}Mo level scheme. By taking advantage of the relatively high Q value of ^{3}He reactions, several new non-yrast states were populated and observed. A standard particle-plus-rotor calculation was performed and used to interpret the experimental level scheme. Special emphasis was placed on identifying complete angular momentum multiplets arising from particle-core coupling.

I. INTRODUCTION

A recent paper from this laboratory[1] reported the success of the (^{3}He,xnγ) reaction in populating non-yrast states in the transitional nucleus ^{99}Ru. The low binding energy of the ^{3}He projectile translates into a higher reaction Q value, thus allowing excitation energy in the final nucleus to be achieved at a lower beam energy than that required for a standard heavy-ion reaction. Since a lower projectile energy means that less orbital angular momentum is brought into the system, the final nucleus is left, after particle emission, in a state well above the yrast curve. From there, decay can proceed to yrast and non-yrast states alike with nearly equal probability.

Ideally one would like to populate all states below a given excitation energy in order to provide an adequate test of the various models of nuclear structure. In a model independent way, one may count the number of states present by considering the coupling of an odd particle to various states of the core. In the weak coupling limit the coupling of an odd particle of angular momentum j to a core state of angular momentum **R** would result in a multiplet of states. For a given **R** and j a complete multiplet would contain states of spin **I**, $|R-j| \leq I \leq R+j$, where the number of states is given by $2j+1$ $(R>j)$ or $2R+1$ $(R<j)$. This counting scheme is by no means limited to weak coupling models. We will show later that multiplets of this sort result naturally from a standard particle-rotor model when the Coriolis interaction is properly included.

In this paper, we report on a study of ^{97}Mo using the same methods as those employed in the ^{99}Ru study. The ^{97}Mo nucleus was chosen because of the relatively wide energy spacing between its three single particle states: the $d_{5/2}$ at 0 keV, the $g_{7/2}$ at 658 keV, and the $h_{11/2}$ at 1437 keV. Since complete angular momentum multiplets are based on each one of these states, wider spacing increases the chances of observing the multiplets with a minimum of interference. Investigations of ^{97}Mo utilizing various techniques have been previously reported,[2–9] but complete multiplets were not observed. While we do observe several new states, experimental difficulties prevent us from making spin assignments for many of the states.

II. EXPERIMENTAL METHODS AND RESULTS

^{97}Mo nuclei were produced by bombarding a $\sim$3 mg/cm^2 thick target of enriched ^{96}Zr with an 11 MeV ^{3}He beam from the Purdue tandem. Target impurities of $\sim$13% contributed to contamination problems which will be discussed later. All gamma-ray measurements were made with Ge(Li) detectors having active volumes of $\sim$60 cm^3 and resolutions of $\sim$1.9 keV full width at half maximum (FWHM) for the 1332.5 keV line from ^{60}Co. A typical singles spectrum is shown in Fig. 1.

A standard set of experiments were performed to provide data for constructing the ^{97}Mo decay scheme. These have been described fully by Whisnant *et al.*,[1] and thus require only a quick summary here. Excitation functions were measured for beam energies of 10, 11, 12, and 14 MeV, and used to determine the most effective beam energy at which to run the other experiments. They also aided in assigning level spins. Angular distributions, measured at 0°, 45°, and 90° with respect to the beam axis, and linear polarizations, measured at 90° with two Ge(Li) detectors configured as a Compton polarimeter, were analyzed together to extract spin information. Finally, $\gamma-\gamma$ coincidences were measured with three Ge(Li) detectors. Coincidence intensities were used to construct the level scheme and to calculate intensities for contaminated transitions.

While the coincidence experiment allowed us to construct the level scheme, problems with the singles experiments precluded the determination of level spins in many cases. If two or more lines of similar intensity are unresolved in energy, their singles peak areas are useless for determining spin information. Nearly half of the γ rays observed in ^{97}Mo suffered from a contamination of 20% or greater. As an example of the difficulties this presented, the "804-keV" complex consisted of no fewer than five transitions, three in ^{97}Mo and two in ^{97}Nb.

While some of the unresolved competing transitions came from ^{97}Mo itself, the majority were produced by other nuclei, as can be seen in Fig. 1. The strongest lines (the 658.3- and 778.2-keV lines) are indeed from ^{97}Mo, but many of the other intense peaks were of unknown origin initially. The subsequent coincidence analysis placed

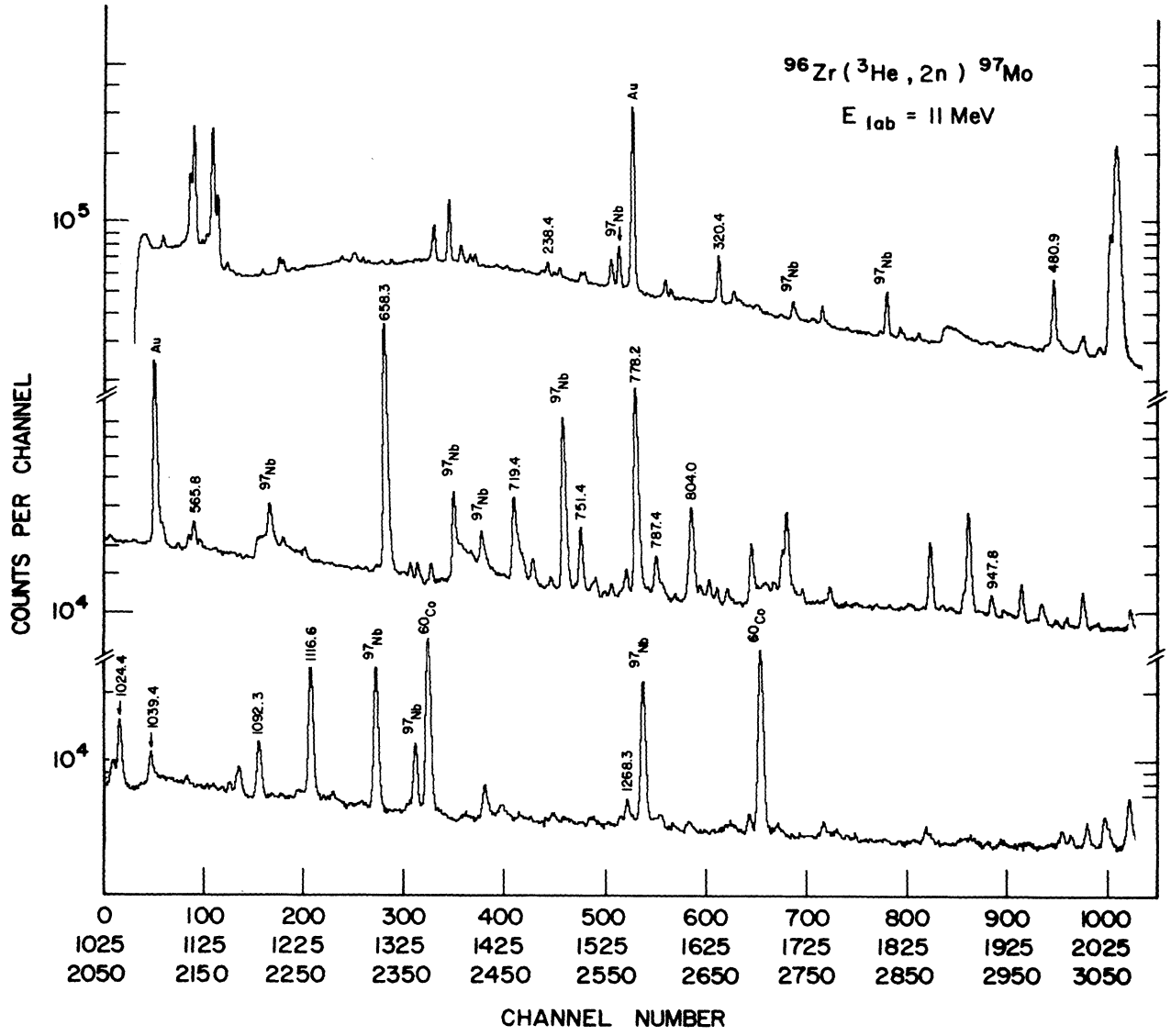

FIG. 1. Typical singles spectrum for the ^{96}Zr(^{3}He, 2nγ)^{97}Mo reaction at a laboratory energy of 11 MeV.

many of these unknown lines in ^{97}Nb, which was produced by the ^{96}Zr(^{3}He,pn) reaction. This reaction channel was the largest factor in the unusual number of unresolved peaks.

In this laboratory the standard method of dealing with transitions for which singles data is useless has been to perform a DCOQ (directional correlation of oriented nuclei referenced to quadrupoles) analysis[1] on the coincidence data. Since coincidence intensities are in general unaffected by unresolved lines from other nuclei, the DCOQ analysis can frequently provide valuable spin information. When applied to our set of data, however, this method failed to produce any useful results. Low intensities, deorientation, the small number of quadrupole transitions, and the absence of long gamma-ray cascades all contributed to the failure.

Of the lines for which an angular momentum analysis was feasible, many had been observed previously, and more accurate measurements have appeared in the literature.[10] While our data confirm previous assignments, we have elected to present the result of the excitation function, angular distribution, and linear polarization analyses only for those new lines where they were of use.

In light-ion-induced fusion reactions the slope of an excitation function is sensitive to the spin of the state that emits the γ ray. Table I lists the slopes of all useful excitation functions, found by fitting lines to the logarithms of the peak areas at the different bombarding energies. The 1117-keV line was used to normalize the other areas at each bombarding energy, and its slope is thus 0 by definition. Since it depopulates a $\frac{9}{2}^+$ state, that spin becomes the zero point. Transitions depopulating states with $I > \frac{9}{2}$ have a positive slope, and those from states with $I < \frac{9}{2}$ have a negative slope. The higher or lower the spin, the more positive or negative the slope. This can be

TABLE I. ^{97}Mo excitation function slopes.

E_γ	I_i	Slope (Error)
238.4	$\frac{5}{2}^+$	−0.183(29)
407.0	$\frac{1}{2}^+$	−0.273(68)
565.8	$(\frac{15}{2}^-)$	0.138(28)
666.2		−0.018(84)
679.5	$\frac{1}{2}^+$	−0.318(65)
751.4	$\frac{11}{2}^+$	0.004(15)
758.4		0.098(105)
790.0		−0.163(88)
821.1		−0.115(112)
924.2		0.157(116)
1127.4		0.435(60)
1268.3	$\frac{7}{2}^+$	−0.126(33)
1515.5	$\frac{9}{2}^+$	−0.018(40)
1565.5	$(\frac{7}{2}^+)$	−0.061(45)

seen in a general way in Table I, where the listed spins are from states of known spin to fix the scale. Poor statistics and complicated feeding patterns (especially for ground state transitions) cause some minor discrepancies, but in general the slopes are as expected.

Table II lists the useful information extracted from the joint analysis of the angular distribution and linear polarization data. As was discussed in detail in the ^{99}Ru paper,[1] nuclear orientations obtained in ^{3}He induced reactions are small, so that the A_{44} coefficients of the standard angular distribution expression are expected to be zero statistically. Thus the A_{22} coefficients were determined by fitting the angular distribution data with A_{44} set to zero. Polarizations were not measured for four out of the seven γ rays listed because of the low γ-ray intensity and the poorer resolution of the polarimeter. Note also that only two mixing ratios are given. These represent a confirmation of a previously measured ratio in the case of the 320-keV transition, and a new value for the 790-keV transition. Spin changes are given in the final column. These are not necessarily determined from the information in the table alone, but represent the final choice for each transition using all available data (excitation functions, level scheme placement, etc.).

Transition intensities were measured by comparing the singles intensity extracted from the angular distribution data to the coincidence intensity for each transition. After computing an average singles to coincidence ratio, it was possible to detect contaminated transitions by virtue of their larger-than-expected singles intensities. The precise nature of the contamination could be determined by searching for coincidences with γ rays from other nuclei. Since coincidence intensities were not available for ground state transitions, their intensities had to be found by subtracting any contaminant intensities measured in the coincidence experiment from the singles intensities.

Table III lists the measured transition intensities and energies. The transition energies are believed accurate to within 0.3 keV, except for the "547"-keV transition, which was buried by the intense Au transition at 547.6 keV. The initial state energy for each transition is included to distinguish between two or more lines of the same energy. An attempt has been made to identify the energy, origin, and intensity of all unresolved contaminants in the last three columns.

III. LEVEL SCHEME

The experimental level scheme for ^{97}Mo is shown in Fig. 2 and tabulated in Table IV. The experimental spins are based on the present series of experiments and on work by other groups published in the literature. Parentheses indicate a preferred but not unique assignment. In Table IV the final column indicates the basis for the spin assignment. Where the present work has not provided new spin information, the adopted spin from Nuclear Data Sheets[10] has been given. In some cases our results have indicated new placements of γ rays reported by other investigators. This also is listed in the final column. Levels with no label in the final column have been seen for the first time in the present work. We observed a total of 19 new levels out of the 41 included in the level scheme.

Several levels in the decay scheme are depopulated by two transitions which do not have a common coincidence, because no transition populating the level was observed. The claim that the initial states of these different transitions are actually the same level is made solely on the basis of energy matches. This is the case for the levels at 1270.8, 1284.5, 1627.3, 1782.8, 1865.0, 1909.0, 1940.0, 2197.3, and 2627.0 keV.

There are four gamma-ray energies for which multiple placement in the ^{97}Mo level scheme is required by coincidence intensities: 705.5, 787.4, 804.0, and 1024.4 keV. One assignment for the 787.4- and both assignments for

TABLE II. New information from angular momentum analysis. The spin change listed is determined from all data.

E_γ	A_{22}	Polarization	Mixing ratio	ΔI
320.4	−0.117(11)	0.255(65)	$0.01 < \delta < 0.07$	−1
666.2	−0.501(89)			−1
758.4	0.155(43)			−2
790.0	−0.039(71)	−0.701(521)	$0.08 < \delta < 0.25$	−1
821.1	0.307(64)			0, +1
924.2	−0.233(88)			0, −1
1281.6	0.147(130)	1.003(1040)		0, −2

TABLE III. Transition intensities.

E_γ (keV)	E_i (keV)	Int.	Unresolved contaminants		
			E (keV)	Nucleus	Int.
238.4	719.4	19(1)			
247.2	1515.5	16(2)			
320.4	1437.0	65(2)			
366.1	1024.4	3(1)			
397.4	1116.6	2(1)	397	^{97}Nb	2
407.0	888.0	9(1)			
428.1	1865.0	5(1)			
458.3	1116.6	3(1)			
480.9	480.9	102(2)	480.8	^{96}Mo	4
			481	^{92}Mo	2
547	1267	4(1)	547.6	^{197}Au	456
548.9	1268.3	4(1)	550.1	^{94}Zr	19
558.1	2073.6	2(1)	558	^{97}Nb	3
565.8	2002.8	20(2)			
658.2	658.2	1000(52)[a]			
666.2	1782.8	7(1)			
679.5	679.5	17(1)			
705.5	2271.0	2(1)	706	^{97}Nb	8
			706	^{97}Mo	1
705.5	2708.3	1(1)	706	^{97}Nb	8
			706	^{97}Mo	2
719.4	719.4	43(2)	719.5	^{96}Mo	61
721.1	721.1	34(1)[b]	721.6	^{96}Mo	
722.8	2725.6	2(1)	722.6	^{98}Mo	28
751.4	1409.6	62(4)	750.5	^{94}Zr	4
758.4	1782.8	10(1)			
778.2	1437.0	7(2)	778.2	^{96}Mo	500
787.4	1268.3	7(1)	787.4	^{98}Mo	28
			787	^{97}Mo	3
787.4	2197.3	3(1)	787.4	^{98}Mo	28
			787	^{97}Mo	7
790.0	1270.8	9(1)	790	^{97}Nb	3
796.3	1515.5	4(1)			
803.6	1284.5	4(1)	804.5	^{97}Nb	
			804	^{97}Nb	15
			804	^{97}Mo	4
			804	^{97}Mo	26
804.0	1692.0	4(1)	804.5	^{97}Nb	
			804	^{97}Nb	15
			804	^{97}Mo	4
			804	^{97}Mo	26
804.4	1921.0	26(3)	804.5	^{97}Nb	
			804	^{97}Nb	15
			804	^{97}Mo	4
			804	^{97}Mo	4
821.1	2258.1	8(1)			
823.4	1940.0	3(1)			
836.9	1556.3	6(1)	837	^{96}Mo	2
840.6	1865.0	6(1)	841	^{96}Mo	2
843.4	2627.0	1(1)	843	^{96}Mo	4
854.6	1512.8	7(2)			
892.6	2813.2	2(1)			
907.9	1627.3	2(1)	908		1
924.2	2040.8	4(1)			
947.8	2357.4	1(1)	948		13
1024.4	1024.4	73(4)	1024	^{97}Mo	8
1024.4	2434.0	8(1)	1024.4	^{97}Mo	73
1039.4	1697.6	16(2)	1039		10
1080.9	2197.3	3(1)	1081	^{97}Nb	5

TABLE III. (*Continued*).

E_γ (keV)	E_i (keV)	Int.	Unresolved contaminants		
			E (keV)	Nucleus	Int.
1092.2	1092.2	21(2)[b]			
1116.6	1116.6	171(2)			
1127.4	2244.0	3(1)	1127	^{96}Mo	2
1148.0	1627.3	5(1)	1147.95	^{97}Nb	250
1189.3	1909.0	2(1)	1189		2
1217.4	2627.0	1(1)			
1251.0	1909.0	2(1)	1251	^{97}Nb	5
1268.3	1268.3	24(2)	1268	^{97}Nb	2
1270.8	1270.8	6(1)[b]			
1281.6	1940.0	3(1)	1282	^{97}Nb	1
1284.5	1284.5	8(1)[b]			
1515.5	1515.5	16(2)			
1565.5	1565.5	21(1)			

[a]Contaminated by β^- decay from ^{97}Nb.
[b]No coincidence window set.

the 1024.4-keV transitions have been observed previously. (See Measurement column in Table IV.) The 804.0-keV energy presents an extraordinarily complex picture, having no fewer than five placements, two in ^{97}Nb and three in ^{97}Mo. Two of the placements in ^{97}Mo have been suggested previously.

Several level spin assignments and transition placements, labeled with a "b" in the Measurement column of Table IV, require elaboration.

The 1267-keV level. The existence of this level was determined by the coincidence between a "547-keV" transition and the 719.2-keV transition. The energy of the level is uncertain because the "547-keV" transition was obscured in the singles measurements by the much more intense 547.6-keV transition from Au. We argue that this is not the 1265.0-keV level observed previously,[9] since the

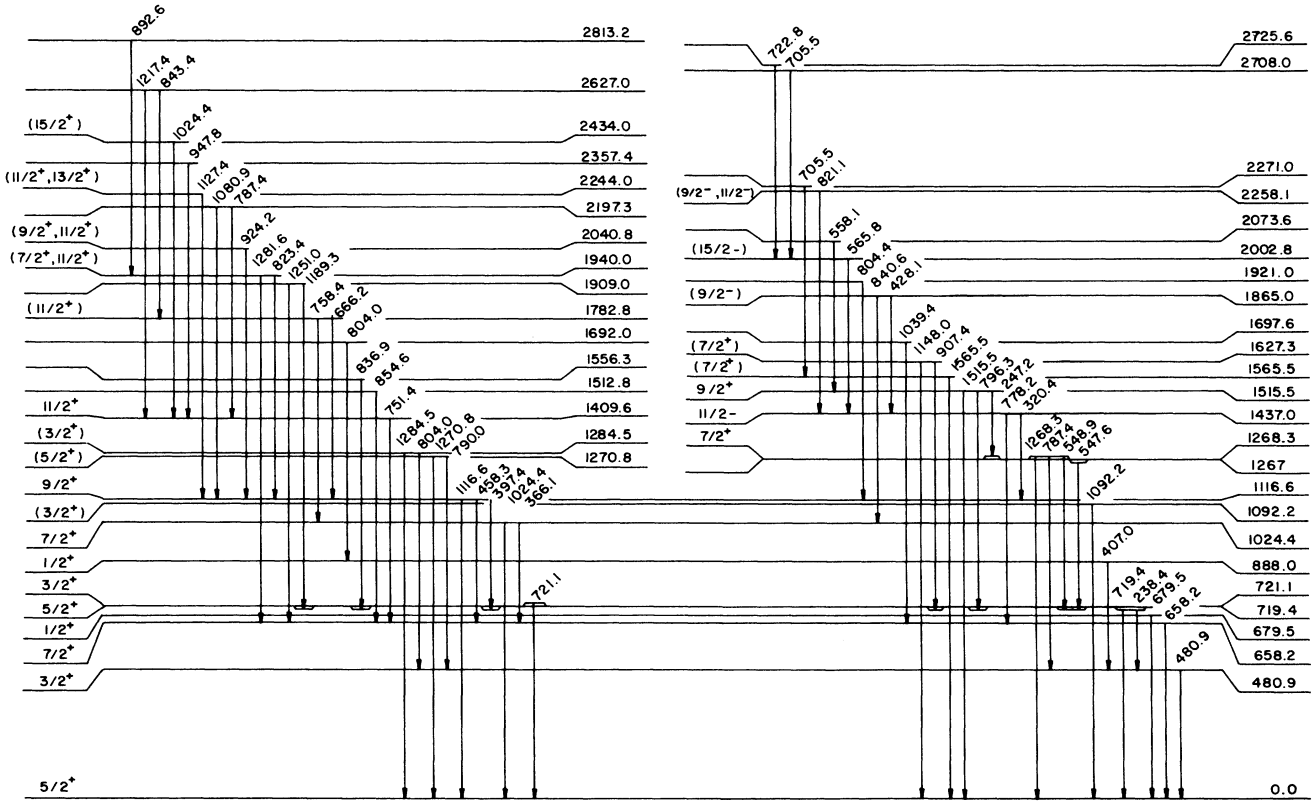

FIG. 2. Decay scheme for ^{97}Mo.

TABLE IV. Level scheme summary. N denotes data from Nuclear Data Sheets (Ref. 10). Footnotes c–e refer to ^{94}Zr(α,nγ)^{97}Mo (Ref. 2) only.

E_i	E_γ	I_i(Expt.)	Measurement	E_i	E_γ	I_i(Expt.)	Measurement
480.9	480.9	$\frac{3}{2}^+$	N	1565.5	1565.5	$(\frac{7}{2}^+)$	a
658.2	658.2	$\frac{7}{2}^+$	N	1627.3	1148.0	$(\frac{7}{2}^+)$	a
679.5	679.5	$\frac{1}{2}^+$	N		907.9		
719.4	719.4	$\frac{5}{2}^+$	N	1692.0	804.0		
	238.4			1697.6	1039.4		a,c
721.1	721.1	$\frac{3}{2}^+$	N	1782.8	758.4	$(\frac{11}{2}^+)$	a,d,b
888.0	407.0	$\frac{1}{2}^+$	N		666.2		
1024.4	1024.4	$\frac{7}{2}^+$	N	1865.0	840.6	$(\frac{9}{2}^-)$	a,c,b
	366.1				428.1		
1092.2	1092.2	$(\frac{3}{2}^+)$	N	1909.0	1251.0		a,c
1116.6	1116.6	$\frac{9}{2}^+$	N		1189.3		
	458.3			1921.0	804.4		N
	397.4			1940.0	1281.6	$(\frac{7}{2}^+, \frac{11}{2}^+)$	N,b
1267	547		b		823.4		
1268.3	1268.3	$\frac{7}{2}^+$	N	2002.8	565.8	$(\frac{15}{2}^-)$	N,b
	787.4			2040.8	924.2	$(\frac{9}{2}^+, \frac{11}{2}^+)$	b
	548.9			2073.6	558.1		
1270.8	1270.8	$(\frac{5}{2}^+)$	b	2197.3	1080.9		
	790.0				787.4		
1284.5	1284.5	$(\frac{3}{2}^+)$	N	2244.0	1127.4	$(\frac{11}{2}^+, \frac{13}{2}^+)$	a,c,b
	803.6			2258.1	821.1	$(\frac{9}{2}^-, \frac{11}{2}^-)$	b
1409.6	751.4	$\frac{11}{2}^+$	N	2271.0	705.5		
1437.0	778.2	$\frac{11}{2}^-$	N	2357.4	947.8		
	320.4			2434.0	1024.4	$(\frac{15}{2}^+)$	N
1512.8	854.6			2627.0	1217.4		
1515.5	1515.5	$\frac{9}{2}^+$	N		843.4		
	796.3			2708.0	705.5		
	247.2			2725.6	722.8		a,e,b
1556.3	836.9			2813.2	892.6		

[a] ^{94}Zr(α,nγ)^{97}Mo (Ref. 2).
[b] Discussed in text.
[c] Observed but not placed.
[d] Placed as in present work, but omitted from final level scheme.
[e] Placement differs from present work.

two states decay in completely different ways.

The 1270.8-keV level. A spin of $(\frac{5}{2}^+)$ is assigned on the basis of the joint angular-distribution/linear-polarization analysis on the 790-keV transition. The small A_{22} and relatively large negative polarization make a spin change of -1 most likely, an assignment which is supported by the 790-keV excitation function. The spin is in parentheses because of the contamination from ^{97}Nb.

The 1782.8-keV level. A large negative A_{22} for the 666-keV transition rules out a spin change of $\Delta I = 0, \pm 2$, leaving only $\frac{11}{2}^+$ and $\frac{7}{2}^+$ as possible spins for the state. The excitation functions for the 666- and 758-keV transitions slightly favor the former spin. This assignment is in disagreement with the adopted value[10] of $\frac{7}{2}^+, \frac{9}{2}^+$. This adopted spin was based on an $L = 4$ transfer in a (d,p) experiment[8] to a level at 1789 keV, which we assume is a different state.

The 1865.0-keV level. This is one of the cases where we infer that a single level exists because of the energy match (better than 0.1 keV) of two independent γ-ray cascades. One cascade is established by a coincidence between the 428- and 320-keV transitions. Our placement of the 428-keV transition differs from that of Mesko *et al.*,[2] who see only the 428-1117 coincidence. The spin assignment is based partly on their angular distribution for the 428-keV transition, which is still valid despite differing placements and is characteristic of a mixed $\Delta I = \pm 1$ or 0 transition. Since the transition populates a known $\frac{11}{2}^-$ state, this restricts the spin to $\frac{9}{2}^-$, $\frac{11}{2}^-$, or $\frac{13}{2}^-$. The second cascade is established by a coincidence between the 840.6- and 1024.4-keV transitions. The 840.6-keV transition feeds a $\frac{7}{2}^+$ state. Since $M2$ or $E3$ transitions are not expected to compete with $M1$ transitions, this leaves us with a most probable spin of $\frac{9}{2}^-$ for the level.

The 1940.0-keV level. A spin choice of $(\frac{7}{2}^+, \frac{11}{2}^+)$ is assigned on the basis of a joint angular distribution/linear polarization analysis of the 1282-keV transition. Because of the large errors and high degree of contamination involved, this assignment is extremely tentative.

The 2002.8-keV level. The existence of this level is based on a coincidence between the 566- and 320-keV transitions. Again, the placement of the 566-keV transition differs from that of Mesko *et al.*,[2] and for the same reasons as the 428-keV transition. Lederer *et al.*[3] support our placement, however, and we use their spin assignment.

The 2040.8-keV level. The excitation function for the 924-keV transition has a positive slope, requiring that $I \geq \frac{9}{2}$. A large negative A_{22} rules out a spin change of $\Delta I = -2$, resulting in a $(\frac{9}{2}^+, \frac{11}{2}^+)$ assignment.

The 2244.0-keV level. The large positive excitation function slope for the 1127-keV transition demands a high spin, even allowing for contamination of the transition. Since the 1127-keV transition feeds a spin $\frac{9}{2}^+$ state, the two highest possibilities are $\frac{11}{2}^+$ and $\frac{13}{2}^+$. Both are given because of the uncertainty caused by the high degree of contamination.

The 2258.1-keV level. Experimentally, the excitation function of the 821-keV transition requires a spin of $I \leq \frac{11}{2}$. The large positive A_{22} for the 821-keV transition rules out a $\Delta I = +2$ spin change, which leaves us with $\frac{9}{2}^-$ and $\frac{11}{2}^-$ as possible spins.

The 2725.6-keV level. The existence of this level is determined by a 723-566-320-keV coincidence. Lederer *et al.*[3] differ in the placement of the 723-keV transition, since they see only a 723-320 coincidence. Our observation makes the existence of their 2160-keV level unlikely.

IV. DISCUSSION

A standard particle-plus-symmetric-rotor calculation was performed for ^{97}Mo as an aid in interpreting our experimental level scheme. As mentioned in the ^{99}Ru paper,[1] this model has been generally successful in the mass-100 region of nuclei. The details of this calculation may be found in papers by Smith and Rickey,[11] and by Popli *et al.*[12] The specific model utilizes a rotational Hamiltonian in the strong coupling limit modified to include a variable moment of inertia.[13] The basis states are thus rotational bands built on Nilsson single particle states,[14] characterized by good K and Ω, the projections of the total angular momentum I and the particle angular momentum j on the symmetry axis. Pairing is treated in the BCS formalism. The Coriolis and recoil terms, which mix these states, were treated to all orders. The parameters used in the present work were basically the same as for the ^{99}Ru work, with small changes. For the positive parity calculation, the values of the Nilsson parameters were $\kappa = 0.07$, $\mu = 0.28$, and the deformation $\delta = 0.12$. The Fermi level and pairing gap were $\lambda = 46.85$ MeV and $\Delta = 1.2$ MeV, respectively, while the variable moment of inertia (VMI) parameters were chosen as $C = 0.1$ and $\mathscr{I}_0 = 0$. Finally, the Coriolis and recoil term matrix elements were multiplied by attenuation factors of 0.9 and 0.8, respectively. For the negative parity calculation, we used $\kappa = 0.0715$, $C = 0.05$, $\delta = 0.1$, and a Coriolis attenuation coefficient of 0.85. All other parameters were the same as for the positive parity calculation.

When the Coriolis interaction is negligible, as for many strongly deformed nuclei, the model predicts regular rotational bands based on Nilsson states. When, however, the Coriolis interaction has large effects, as for slightly deformed nuclei like ^{97}Mo, the final states resemble the particle-core multiplets discussed earlier in that they normally contain a dominant R and j rather than a dominant Ω. For ^{97}Mo the possible j values are $\frac{1}{2}$, $\frac{3}{2}$, $\frac{5}{2}$, $\frac{7}{2}$, and $\frac{11}{2}$ for the $s_{1/2}$, $d_{3/2}$, $d_{5/2}$, $g_{7/2}$, and $h_{11/2}$ orbits, respectively. The number of states with the same dominant R and j is that expected for a multiplet, as are the spins. The average energy of one of these groups increases with R as expected from the core. We thus use the descriptive label "multiplet" rather than "band" in making an association between groups of calculated and observed states. However, the label of R and j for a particular state is not meant to imply that its energy and decay properties can be estimated easily by weak-coupling arguments. The wave function can have substantial admixtures of other R and j values, and the calculated properties come from the complete rotational description.

The major question of identification involves establishing a correspondence between calculated and experimental levels. This cannot be done on the basis of energies and angular momenta alone, since several states of a given angular momentum can have similar energies. As a result, we use branching ratios to complete the identification. We require that a state both decay and be fed as expected, providing a much more definite correspondence than a simple energy match.

The results of the calculation are listed in Table V. The first four columns are self-explanatory. In the fifth, we list the experimental energies of all gamma rays depopulating the states. (These energies were used in the calculation of transition properties as well.) When an entry is given for a transition predicted by the calculation but not observed experimentally, the energy has been calculated from the experimental initial and final state energies.

In the sixth and seventh columns of Table V, we compare the experimental and theoretical branching ratios for each gamma ray. The experimental values are calculated from the transition intensities given in Table III. An entry is given for each gamma ray observed, regardless of how weak the branch. Entries are also included for unobserved transitions predicted by the calculation to have a ratio of greater than or equal to 5%. In the final two columns, we give the dominant R and j values of the calculated wave function for the initial state.

For all but one of the states included in Table V the dominant j value is calculated to be either $j = \frac{5}{2}$, $\frac{7}{2}$, or $\frac{11}{2}$, as would be expected from the position of the Fermi surface. States with dominant $j = \frac{3}{2}$ are predicted at higher excitation energies. There are, however, substantial $j = \frac{3}{2}$ components predicted for states in the table. For example, the calculated wave function of the second $\frac{1}{2}^+$ state at 888.0 keV has a 30% $j = \frac{3}{2}$ component, even

TABLE V. Calculation results.

E_i (keV)		I_i^π	I_f^π	E_γ (keV)	Branching ratio		R	j (Initial)
Expt.	Theor.				Expt.	Theor.		
480.9	400	$\frac{3}{2}^+$	$\frac{5}{2}^+$	480.9	1.00	1.00	2	$\frac{7}{2}$
658.2	431	$\frac{7}{2}^+$	$\frac{5}{2}^+$	658.2	1.00	0.98	0	$\frac{7}{2}$
679.5	646	$\frac{1}{2}^+$	$\frac{5}{2}^+$	679.5	1.00	0.89	0	$\frac{1}{2}$
			$\frac{3}{2}^+$	198.6	0.00	0.11		
719.4	1144	$\frac{5}{2}^+$	$\frac{5}{2}^+$	719.4	0.81	0.82	2	$\frac{5}{2}$
			$\frac{3}{2}^+$	238.4	0.19	0.18		
721.1	544	$\frac{3}{2}^+$	$\frac{5}{2}^+$	721.1	1.00	0.95	2	$\frac{5}{2}$
			$\frac{3}{2}^+$	240.2	0.00	0.05		
888.0	974	$\frac{1}{2}^+$	$\frac{3}{2}^+$	407.0	1.00	0.57	2	$\frac{5}{2}$
			$\frac{5}{2}^+$	888.0	0.00	0.41		
1024.4	1019	$\frac{7}{2}^+$	$\frac{5}{2}^+$	1024.4	0.98	0.80	2	$\frac{5}{2}$
			$\frac{7}{2}^+$	366.1	0.02	0.00		
			$\frac{5}{2}^+$	305.0	0.00	0.20		
1116.6	1106	$\frac{9}{2}^+$	$\frac{5}{2}^+$	1116.6	0.97	0.97	2	$\frac{5}{2}$
			$\frac{5}{2}^+$	397.4	0.02	0.00		
			$\frac{7}{2}^+$	458.3	0.01	0.03		
1270.8	1358	$\frac{5}{2}^+$	$\frac{3}{2}^+$	790.0	0.60	0.07	2	$\frac{7}{2}$
			$\frac{5}{2}^+$	1270.9	0.40	0.68		
			$\frac{5}{2}^+$	551.5	0.00	0.24		
1284.5	1576	$\frac{3}{2}^+$	$\frac{5}{2}^+$	1284.5	0.67	0.91	2	$\frac{7}{2}$
			$\frac{3}{2}^+$	804.0	0.33	0.08		
1409.6	1446	$\frac{11}{2}^+$	$\frac{7}{2}^+$	751.4	1.00	1.00	2	$\frac{7}{2}$
1437.0	1437	$\frac{11}{2}^-$	$\frac{9}{2}^+$	320.4	0.90	1.00	0	$\frac{11}{2}$
			$\frac{7}{2}^+$	778.2	0.10	0.00		
1697.6	1927	$\frac{9}{2}^+$	$\frac{7}{2}^+$	1039.4	1.00	0.60	2	$\frac{7}{2}$
			$\frac{5}{2}^+$	978.2	0.00	0.29		
			$\frac{9}{2}^+$	581.0	0.00	0.08		
1782.8	2129	$\frac{11}{2}^+$	$\frac{7}{2}^+$	758.4	0.59	0.71	4	$\frac{5}{2}$
			$\frac{9}{2}^+$	666.2	0.41	0.24		
1865.0	1995	$\frac{9}{2}^-$	$\frac{7}{2}^+$	840.6	0.55	0.42	2	$\frac{11}{2}$
			$\frac{11}{2}^-$	428.1	0.45	0.41		
			$\frac{7}{2}^+$	1206.8	0.00	0.16		
1920.6	2277	$\frac{13}{2}^+$	$\frac{9}{2}^+$	804.0	1.00	0.91	4	$\frac{5}{2}$
			$\frac{11}{2}^+$	137.8	0.00	0.06		
1940.0	2252	$\frac{7}{2}^+$	$\frac{7}{2}^+$	1281.6	0.50	0.17	2	$\frac{7}{2}$
			$\frac{9}{2}^+$	823.4	0.50	0.41		
			$\frac{3}{2}^+$	1459.1	0.00	0.24		
			$\frac{5}{2}^+$	1220.6	0.00	0.12		
			$\frac{7}{2}^+$	915.6	0.00	0.06		
2002.8	1995	$\frac{15}{2}^-$	$\frac{11}{2}^-$	565.8	1.00	0.99	2	$\frac{11}{2}$
2434.0	2490	$\frac{15}{2}^+$	$\frac{11}{2}^+$	1024.4	1.00	1.00	4	$\frac{7}{2}$
2627.0	2886	$\frac{13}{2}^+$	$\frac{11}{2}^+$	1217.4	0.50	0.50	4	$\frac{7}{2}$
			$\frac{11}{2}^+$	843.4	0.50	0.03		
			$\frac{9}{2}^+$	929.4	0.00	0.42		
			$\frac{13}{2}^+$	706.4	0.00	0.05		
2708.3	2921	$\frac{19}{2}^-$	$\frac{15}{2}^-$	705.5	1.00	1.00	4	$\frac{11}{2}$
2725.6	3283	$\frac{17}{2}^-$	$\frac{15}{2}^-$	722.8	1.00	0.98	4	$\frac{11}{2}$
2813.2	4001	$\frac{17}{2}^+$	$\frac{13}{2}^+$	892.6	1.00	1.00	6	$\frac{5}{2}$

though its dominant component is $j=\frac{5}{2}$. The lowest $\frac{1}{2}^+$ state at 679.5 keV is predicted to be dominantly (53%) $j=\frac{1}{2}$ and $R=0$, which is consistent with the measured (d,p) spectroscopic factor of $C^2S=0.94$.[8] Again the calculated wave function is mixed, and contains a 31% $j=\frac{5}{2}$ component. Mixtures of this magnitude are in fact typical of many of the calculated wave functions for positive parity states in the table.

Based on this interpretation, the extent of non-yrast population can be evaluated. We have observed two complete $R\simeq 2$ multiplets, the $d_{5/2}$ and $g_{7/2}$, and three out of the five $h_{11/2}$ $R\simeq 2$ multiplet states. The two highest spin members of each of the three $R\simeq 4$ multiplets have also been observed, together with the highest spin member of the $d_{5/2}$ $R\simeq 6$ multiplet. The missing members of the various multiplets all reflect the fact that low spin states become increasingly non-yrast in nature as excitation energy increases, and are thus correspondingly more difficult to populate.

Overall, the model does a reasonably good job of reproducing the experimental states, with the notable exception of the second $\frac{5}{2}^+$ state at 719 keV. This problem with the lowest $\frac{5}{2}^+$ states has been observed in neighboring odd-neutron nuclei, and we suspect that it is due to the simplified treatment of pairing. There is also a tendency for the model to overestimate the energies of states at higher excitation energies, as is seen for the $R=4$ and $R=6$ states. This is due to limitations in the VMI treatment of the moment of inertia.

There is no reason why multiplets should not also arise from the coupling of single particle states to the $0^{+'}$ and $2^{+'}$ states of the core, assumed to be patently non-rotational. Multiplet states based on these excitations would obviously not be reproduced by our particle-plus-rotor calculation. In our experiment, we see a total of fifteen states, ranging in energy from 1092 keV to 2357 keV, for which the model is unable to account. Seven of these have at least partial spin assignments, and nine are new states. We of course cannot explicitly identify these states as members of the non-rotational multiplets. They are good candidates, however, and should be considered in any attempt to develop a more complete model.

Our results should be compared to those obtained by Whisnant *et al.*[1] for ^{99}Ru, since that nucleus also has 55 neutrons. The level schemes are similar, but the energy spacings between states are smaller in ^{99}Ru. This can be seen in the differences in energy between the three $R\simeq 0$ bandheads in the two nuclei. For ^{97}Mo, the bandheads are the $\frac{5}{2}^+$, $\frac{7}{2}^+$, and $\frac{11}{2}^-$ states at 0 keV, 658 keV, and 1437 keV, respectively. For ^{99}Ru, the same states are at 0 keV, 341 keV, and 1070 keV. The larger spacings for ^{97}Mo reflect the fact that it is two protons closer to a semiclosed shell at $Z=40$.

Complete $R\simeq 2$ multiplets are populated in both nuclei, and are well described by the model. In general, the correspondence between calculation and experiment is somewhat poorer for ^{97}Mo, possibly reflecting the less rotational nature of nuclei near closed shells. The extent of non-yrast state population is also less in ^{97}Mo. Whisnant *et al.* observe all of the $h_{11/2}$ $R\simeq 2$ states as well as nearly complete $d_{5/2}$ and $g_{7/2}$ $R\simeq 4$ multiplets. Our failure to observe as many non-yrast states was most probably a consequence of the high degree of contamination present in our spectra which no doubt obscured weak lines that otherwise would have been seen.

V. CONCLUSIONS

Taken together, the results of the experiments on ^{99}Ru and ^{97}Mo clearly indicate the effectiveness of ^{3}He reactions in populating non-yrast states. The unusual amount of contamination in the ^{97}Mo experiments made it difficult to extract adequate spin information. New experimental techniques which could select the desired reaction channel are clearly desirable. The observation of complete angular momentum multiplets has provided a further test for the rotational model, which continues to produce an accurate, albeit partial picture of slightly deformed nuclei. The additional observation of several apparently non-rotational states should be helpful in developing a more complete model.

This work was partially supported by the National Science Foundation.

*Present address: Department of Physics, Kansas State University, Manhattan, KS 66506.

†Present address: Texas Instruments, Dallas, TX 75265.

[1] C.S. Whisnant, K.D. Carnes, R.H. Castain, F.A. Rickey, G.S. Samudra, and P.C. Simms, Phys. Rev. C **34**, 443 (1986).

[2] L. Mesko, A. Nilsson, S.A. Hjorth, M. Brenner, and O. Holmlund, Nucl. Phys. **A181**, 566 (1972).

[3] C.M. Lederer, J.M. Jaklevic, and J.M. Hollander, Nucl. Phys. **A169**, 489 (1971).

[4] J. Barrette, M. Barrette, R. Haroutunian, G. Lamoureux, S. Monaro, and S. Markiza, Phys. Rev. C **11**, 171 (1975).

[5] B. Arad, W.V. Prestwich, A.M. Lopez, and K. Fritze, Can. J. Phys. **48**, 1378 (1970).

[6] H. Behrens and F. Brodt, Nucl. Phys. **A150**, 269 (1970).

[7] K. Rimawi and R.E. Chrien, Phys. Rev. C **15**, 1271 (1977).

[8] L.R. Medsker and J.L. Yntema, Phys. Rev. C **9**, 664 (1974).

[9] W. Dietrich, G.C. Madueme, L. Westerberg, and A. Backlin, Phys. Scr. **12**, 271 (1975).

[10] B. Haesner and P. Luksch, Nucl. Data Sheets **46**, 607 (1985).

[11] H.A. Smith, Jr. and F.A. Rickey, Phys. Rev. C **14**, 1946 (1976).

[12] Rakesh Popli, F.A. Rickey, L.E. Samuelson, and P.C. Simms, Phys. Rev. C **23**, 1085 (1981).

[13] M.A.J. Mariscotti, G. Scharff-Goldhaber, and B. Buck, Phys. Rev. **178**, 1864 (1969).

[14] S.G. Nilsson, K. Dan. Vidensk. Selsk. Mat.-Fys. Medd. **29**, No. 16 (1955).